A modified carrier-to-code leveling method for retrieving ionospheric observables and detecting short-term temporal variability of receiver differential code biases

Baocheng Zhang[1*], Peter J.G. Teunissen[2, 3], Yunbin Yuan[1], Xiao Zhang[1], Min Li[1]

E-mail: b.zhang@whigg.ac.cn

1. State Key Laboratory of Geodesy and Earth's Dynamics, Institute of Geodesy and Geophysics, Chinese Academy of Sciences, Wuhan, China
2. Global Navigation Satellite System (GNSS) Research Centre, Curtin University, Perth, Australia
3. Geoscience and Remote Sensing, Delft University of Technology, Delft, The Netherlands

Abstract

Sensing the ionosphere with the Global Positioning System (GPS) involves two sequential tasks, namely, the ionospheric observable retrieval and the ionospheric parameter estimation. A prominent source of error has long been identified as short-term variability in receiver Differential Code Bias (rDCB). We modify the Carrier-to-Code Leveling (CCL), a method commonly used to accomplish the first task, through assuming rDCB to be unlinked in time. Aside from the ionospheric observables, which are affected by, among others, the rDCB at one reference epoch, the Modified CCL (MCCL) can also provide the rDCB offsets with respect to the reference epoch as by-products. Two consequences arise. First, MCCL is capable of excluding the effects of time-varying rDCB from the ionospheric observables, which, in turn, improves

the quality of ionospheric parameters of interest. Second, MCCL has significant potential as a means to detect between-epoch fluctuations experienced by rDCB of a single receiver.

Keywords

Global Positioning System (GPS); Ionosphere; Vertical Total Electron Content (vTEC); Receiver Differential Code Bias (rDCB); Modified Carrier-to-Code Leveling (MCCL)

Introduction

Since its first operation in 1978, Global Positioning System (GPS) has proven to be an effective sensor for monitoring the ionosphere with wide spatial coverage and high temporal resolution (Jorgensen, 1978; Mannucci et al. 1993; Hernández-Pajares et al. 1999; Liu and Gao, 2004; Li et al. 2015). The vertical Total Electron Content (vTEC) accounts for one of the most important ionospheric parameters that GPS can provide (Brunini and Azpilicueta, 2009; Brunini and Azpilicueta, 2010), since its use in a variety of applications is continuously expanding (E Sardon et al. 1994; Artru et al. 2005; Dautermann et al. 2007; Park et al. 2011; Komjathy et al. 2012; Dettmering et al. 2014; Gulyaeva et al. 2014). This motivates the International GNSS Service (IGS) to regularly produce the snapshots of the global vTEC in the form of Global Ionosphere Maps (GIM) (Mannucci et al. 1998; Feltens, 2003; Hernández-Pajares et al. 2009).

In order to acquire vTEC from dual-frequency GPS data, one needs to carry out two tasks sequentially (Dyrud et al. 2008; Brunini et al. 2011). The

first task concerns the combination of geometry-free code and phase measurements through the Carrier-to-Code Leveling (CCL), so as to retrieve on an arc-by-arc basis the ionospheric observables (Ciraolo et al. 2007); this observable, related to the slant TEC (sTEC) along the satellite-receiver line-of-sight, is affected by Differential Code Biases (DCB) that can further be separated into those introduced by the satellite (sDCB) and those introduced by the receiver (rDCB) (Esther Sardon et al. 1994; Coster et al. 2013). In the second task, one common practice is to turn to the thin-layer ionosphere model to remove DCB from ionospheric observables, leaving only the sTEC, from which one can readily derive the vTEC by using a mapping function (Brunini et al. 2011; Zus et al. 2014; Li et al. 2017).

There exist a number of sources of error to which the vTEC results are particularly prone. Unlike the sDCB that normally exhibit a high degree of stability day to day (Esther Sardon et al. 1994; Xue et al. 2016; Zhong et al. 2016), the rDCB can vary dramatically on time-scales of hours or less, due mainly to temperature effects (Ciraolo et al. 2007; Brunini and Azpilicueta, 2010; Coster et al. 2013; Kao et al. 2013); this variability not only introduces the leveling errors up to a few TEC units (TECu) to the ionospheric observables (Ciraolo et al. 2007), but is also partially responsible for the misspecification errors in the thin-layer ionosphere model (Brunini and Azpilicueta, 2010), which usually treats DCB as constants for a period of time of at least one day. It is worth mentioning that, misspecification errors can occur also because the mapping function and the mathematical representation of vTEC are always imperfect (Mannucci et al. 1998; Komjathy et al. 2005).

To deal with the leveling errors induced by time-varying rDCB, extensive

efforts have been devoted to the development of three alternative methods to the CCL. The first method relies solely on the geometry-free phase measurements, thereby giving rise to ionospheric observables into which arc-dependent ambiguities enter (Brunini and Azpilicueta, 2009). This method does not perform consistently better than CCL, since it requires the estimation of a high number of ambiguities instead of a minor number of DCB in the thin-layer ionosphere model. The second method employs Precise Point Positioning (PPP), retrieving ionospheric observables from code and phase measurements corrected by precise satellite orbits and clocks externally provided (Zhang et al. 2012). As compared to CCL, PPP can yield ionospheric observables with exactly the same interpretation but reduced leveling errors, owing to its exploitation of a priori knowledge about the geometric effects. In the third method, termed integer leveling (Banville and Langley, 2011; Banville et al. 2012), one attempts to fix the estimable ambiguities to integers and then apply them to geometry-free phase measurements, resulting in ionospheric observables that contain receiver- and satellite-specific biases (which are DCB-like) and are free from leveling errors. We remark that, the common disadvantage of the latter two methods is their dependency on the availability of precise satellite products including orbits, clocks and phase biases, which may limit their usefulness in the everyday practice.

The aim of this contribution is to eliminate the adverse impact of the variability of rDCB on the determination of vTEC in an effective and simple manner. For this, we propose to modify the CCL by allowing the rDCB to change freely over time, leading to a Modified CCL (MCCL) of considerable interest. Roughly speaking, MCCL is much less demanding than PPP or

integer leveling, in the sense that it does not require the acquisition of precise satellite products from an external provider. At the same time, MCCL, in contrast with the original CCL, is advantageous in two respects. First, it avoids the introduction of leveling errors due to short-term variations in rDCB into the ionospheric observables, whose interpretation now becomes a combination of the sTEC, the sDCB and the rDCB at one reference (usually the first) epoch. Second, it enables the provision of rDCB offsets (with respect to the reference epoch) as by-products. Consider the fact that, characterization of the variability of rDCB remains an area of active investigation within the ionospheric community (Coster et al. 2013; Hauschild and Montenbruck, 2016; Wanninger et al. 2017; Zhang et al. 2017). One customary technique for meeting this need employs two receivers creating a zero or a short baseline, allowing one to study the variability only for Between-Receiver DCB (BR-DCB) (Zhang and Teunissen, 2015). In contrast, MCCL can be more promising because of its ability to disclose between-epoch variations exhibited by rDCB of a single receiver.

Methods

In an attempt to make this paper self-contained, we begin by outlining the existing technologies that are related to our work. We then present in detail the MCCL proposed, focusing primarily on the development of its functional model in the framework of S-system theory, and finish with a discussion.

Related technologies

We start with the CCL, proceed to the thin-layer ionosphere model, and end

with the BR-DCB estimation method.

Carrier-to-Code Leveling (CCL)

The system of geometry-free code and phase observation equations, serving as a point of departure, reads (Leick et al. 2015),

$$\begin{aligned} p_r^s(i) &= d_r - d^s + \iota_r^s(i) \\ \phi_r^s(i) &= a_r^s - \iota_r^s(i) \end{aligned} \tag{1}$$

with $p_r^s(i)$ and $\phi_r^s(i)$ the geometry-free code and phase observables associated with receiver r, satellite s and epoch i. d_r and d^s denote, respectively, the rDCB and the sDCB. $\iota_r^s(i)$ denotes the first-order effect of the sTEC on $p_r^s(i)$. a_r^s denotes the real-valued ambiguity. Whereas $\iota_r^s(i)$ can vary between epochs, the remaining parameters are constant over time; this is the usual assumption that the CCL makes.

Let us consider a continuous arc that consists of a total of t epochs. The use of the CCL for ionospheric observable retrieval involves two interrelated tasks. The first task is to determine the so-called leveling constant by (weighted) averaging of $p_r^s(i) + \phi_r^s(i)$ over t epochs. This constant, denoted using c, amounts to $d_r - d^s + a_r^s$. The second task, then, is to subtract $\phi_r^s(i)$ from c, thereby giving rise to a set of ionospheric observables, which read,

$$\bar{\iota}_r^s(i) = \iota_r^s(i) + d_r - d^s \tag{2}$$

for $i = 1 \cdots t$. It is interesting to note that, the $p_r^s(i)$ and the $\bar{\iota}_r^s(i)$ are two

different quantities, but they have the same interpretation.

The presence of errors in $\overline{\iota}_r^s(i)$, called leveling errors, often becomes evident when d_r show significant short-term variations or $p_r^s(i)$ are subject to severe multipath effects (Ciraolo et al. 2007). This is because neither the rDCB variability nor the code multipath can be fully averaged out, especially for a short arc, resulting in a bias in c that eventually enters $\overline{\iota}_r^s(i)$. In order to assess the magnitude of the leveling errors, one typical way is to perform the co-location experiment (Ciraolo et al. 2007; Brunini and Azpilicueta, 2009; Khodabandeh and Teunissen, 2016), consisting in the comparison of ionospheric observables from a couple of receivers so close that the sTEC measured by them ought to be the same. Would the leveling errors be absent, the between-receiver single-differenced ionospheric observables, interpreted as the BR-DCB, would take one common value, irrespective of the arcs to which they pertain. In this way, the between-arc discrepancies allow assessing the magnitude of the leveling errors.

Thin-layer ionosphere model

Isolation of the vTEC, the sDCB and the rDCB from the ionospheric observables can rely upon the thin-layer ionosphere model, approximating the whole ionosphere with a spherical shell of infinitesimal thickness (Schaer, 1999). At the point where the satellite-receiver line-of-sight pierces the shell, called the ionospheric penetration point (IPP), we convert the sTEC $\iota_r^s(i)$ to the vTEC $v_r^s(i)$ by means of a mapping function $m_r^s(i)$, which reads (Brunini and Azpilicueta, 2010),

$$\frac{v_r^s(i)}{\iota_r^s(i)} = \frac{1}{m_r^s(i)} = \sqrt{1-\left(\frac{R}{R+h}\right)^2 \cdot \cos^2\left[e_r^s(i)\right]} \tag{3}$$

where R is the radius of the Earth (6371.395 km), h is the height of the shell (450 km) and $e_r^s(i)$ is the line-of-sight ($s-r$) elevation angle at epoch i.

Next we mathematically represent the spatial and temporal variability of the $v_r^s(i)$. There exist many possibilities for this, but here we opt for a simple one, which reads (Li et al. 2015),

$$\begin{aligned} v_r^s(i) &= f_i\left(E_{ab}, C_k, S_k\right) \\ &= \sum_{a=0}^{2}\sum_{b=0}^{2}\left\{E_{ab}\cdot x^a \cdot y^b\right\} + \sum_{k=1}^{4}\left\{C_k \cdot \cos\left(k\cdot y\right) + S_k \cdot \sin\left(k\cdot y\right)\right\} \end{aligned} \tag{4}$$

with E_{ab}, C_k and S_k the unknown coefficients of the polynomial function chosen and a, b the orders, and where $x = \mu_{IPP} - \mu_{REC}$ and $y = \frac{2\pi\left(t_i - 14\right)}{24}$, μ being the geomagnetic latitude and t_i being the local time; two sub-indices IPP and REC refer, respectively, to the IPP and receiver locations.

Inserting Equations (3), (4) into Equation (2) gives,

$$\overline{\iota}_r^s(i) = m_r^s(i)\cdot f_i\left(E_{ab}, C_k, S_k\right) + d_r - d^s \tag{5}$$

where $\overline{\iota}_r^s(i)$ encompasses now a vector of ionospheric observables at multiple epochs from a single (or multiple) receiver(s). This linear system of equations is solvable by weighted least squares using a zero-mean constraint on the sDCB (Wang et al. 2016), thus yielding the estimates of the coefficients, as well as of the rDCB and sDCB (denoted, respectively, by $\widehat{d}_r$ and $\widehat{d}^s$). More explicitly, this constraint condition imposed assumes that the sum of the sDCB of all satellites in view is equal to zero, thus helpful in eliminating the

rank deficiency (of size one) occurring between the rDCB and the sDCB. Note also that, the choice of the constraint is not unique; there are many possibilities. To follow the IGS convention, we have chosen to use the zero-mean constraint in this work. It then becomes straightforward to compute the vTEC at each IPP as

$$\hat{v}_r^s(i) = \frac{1}{m_r^s(i)} \cdot \left[\bar{\iota}_r^s(i) - \hat{d}_r + \hat{d}^s \right] \tag{6}$$

with $\hat{v}_r^s(i)$ the computed values for the vTEC.

Estimation of between-receiver differential code biases (BR-DCB)

Consider that two receivers (called A and B) create a short or a zero baseline. Differencing $p_A^s(i)$ and $p_B^s(i)$, two geometry-free code observations from satellite s collected simultaneously by A and B at epoch i, cancels the sTEC as well as the sDCB and gives,

$$p_{AB}^s(i) = d_{AB} \tag{7}$$

with $p_{AB}^s(i) = p_A^s(i) - p_B^s(i)$ and $d_{AB} = d_A - d_B$ the BR-DCB.

Equation (7) allows the estimation of the BR-DCB from a single epoch of between-receiver single-differenced, geometry-free code observations measured by all satellites in common view. The epoch-by-epoch estimates of the BR-DCB so obtained can be useful in the later experiments.

Modified Carrier-to-Code Leveling (MCCL)

As stated earlier, the MCCL differs from the CCL in that it assumes the rDCB to be time-varying rather than time-invariant. With this in mind, we re-write

Equation (1) as,

$$\begin{aligned} p_r^s(i) &= d_r(i) - d^s + \iota_r^s(i) \\ \phi_r^s(i) &= a_r^s - \iota_r^s(i) \end{aligned} \tag{8}$$

with $d_r(i)$ the rDCB newly-defined and allowed to change between epochs.

Equation (8), which forms the basis for the development of the functional model of the MCCL, represents a rank-deficient system, implying that not all parameters are unbiasedly estimable, but only combinations of them. By means of reparametrization (Teunissen, 1985), we make this system full-rank by first identifying the types of rank deficiencies and then choosing a minimum set of parameters as datum. These datum parameters, also referred to as S-basis or minimum constraints, are usually fixed to their a priori known values (or simply zero) and not estimated. Moreover, the number of datum parameters equals the size of the rank deficiency.

The first type of rank deficiencies, whose size is the same as the number of satellites, occurs between d^s, $\iota_r^s(i)$ and a_r^s. One solution consists of choosing d^s, namely sDCB, as datum. The second type of rank deficiencies, occurring between $d_r(i)$, $\iota_r^s(i)$ and a_r^s, is of size one (recall that we consider only the case of a single receiver).We solve this by further choosing $d_r(1)$, the rDCB associated with the first (reference) epoch $i=1$, as datum. We have up to this point eliminated the rank deficiencies, resulting in the full-rank version of Equation (8), which reads,

$$\begin{aligned} p_r^s(i) &= \bar{d}_r(i) + \tilde{\iota}_r^s(i) \\ \phi_r^s(i) &= \bar{a}_r^s - \tilde{\iota}_r^s(i) \end{aligned} \tag{9}$$

where

$$\begin{aligned}\bar{d}_r(i) &= d_r(i) - d_r(1)\\ \tilde{\iota}_r^s(i) &= \iota_r^s(i) + d_r(1) - d^s\\ \bar{a}_r^s &= a_r^s + d_r(1) - d^s\end{aligned} \tag{10}$$

with $\bar{d}_r(i)$ the estimable rDCB, $\tilde{\iota}_r^s(i)$ the estimable sTEC and $\bar{a}_r^s$ the estimable ambiguities.

As far as Equations (9), (10) are concerned, two remarks are in order.

First, one can interpret $\bar{d}_r(i)$ as rDCB offsets, that is, a series of original rDCB $d_r(i)$ shifted with respect to the first one $d_r(1)$. Note that, $\bar{d}_r(i)$ are inestimable at the first epoch $i=1$, owing to the fact that $\bar{d}_r(1)=0$. The estimability of $\bar{d}_r(i)$ for $i>1$ enables the direct detection of between-epoch fluctuations, if any, in the rDCB. Since the redundancy is defined as the number of observations minus the number of parameters estimable, the multi-epoch redundancy of the MCCL model is less than that of the CCL model by $t-1$, with t the number of epochs.

Second, $\tilde{\iota}_r^s(i)$, ionospheric observables that MCCL can provide, contain, among others, the rDCB at the first epoch $d_r(1)$, and thus are immune to leveling errors due to possible short-term variations of rDCB. When estimating the vTEC from this ionospheric observable by means of the thin-layer ionosphere model (cf. Equation 5), the d_r gets replaced by $d_r(1)$ whist the d^s remains unchanged. Thus, it becomes reasonable to assume that $d_r(1)$ does not alter over time, as is actually the case. In this way, one can avoid misspecification errors that can arise when proper handling of the rDCB variability is not in place.

Results

In this section, we first describe the setup of the experiments, including the experimental environment and the datasets. Following this is a summary of the experimental results.

Experimental setup

For our analysis we selected two sets of GPS data, each measured by three co-located receivers over three consecutive days, with four observation types (C1, P2, L1, L2) and a 30-second interval (see Table 1 for detailed characteristics). There are two interesting points to note from Table 1. First, ALGO, ALG2 and ALG3 are each equipped with a single antenna, implying that they can create a total of three short baselines, with lengths between about 70 meters and 150 meters. Second, LPGB and LPGR, two identical receivers, create a zero baseline, because they were connected to a common antenna, located approximately five meters away from the antenna of the LPGS receiver. We further point out that, whilst the second set of data was used by (Ciraolo et al. 2007) to prove that rDCB can exhibit significant within-day variations, resulting in the presence of the leveling errors, the first set of data was used by (Banville and Langley, 2011) to demonstrate that the integer leveling method is able to remove most of the leveling errors.

We processed each set of GPS data as follows.

First, for each pair of receivers we computed the epoch-by-epoch estimates of BR-DCB, making it possible to identify those receivers whose rDCB can show a significant change over a period of one day. With the

information so gained, it enables us to assess the validity of the MCCL for detecting between-epoch variations in rDCB of a single receiver.

Second, we retrieved two sets of ionospheric observables, with one set using the CCL and the other using the MCCL. Then we applied the thin-layer ionosphere model to each set, resulting in the corresponding vTEC values. A thorough analysis of these results shall demonstrate that the MCCL is superior to the CCL, owing to its ability to circumvent the leveling and/or misspecification errors introduced by the variability of the rDCB.

In our data processing, we apply a cut off elevation angle of 20 degrees, aiming to exclude particularly noisy GPS data. To construct the stochastic model, we opt for the use of an elevation-dependent weighting of the observations, in which we empirically set the zenith-referenced standard deviation to 30 centimeters for the code observables and to 0.3 centimeters for the phase observables. We base the calculation of elevation angles on the satellite positions computed using the broadcast orbits, and the receiver positions assumed to be a-priori known.

On the short-term variations of rDCB

Figure 1 shows the epoch-by-epoch estimates of BR-DCB for three pairs of receivers (ALG2—ALGO, blue line; ALG3—ALGO, red line; ALG3—ALG2, yellow line) and for three days (16, 17 and 18 of 2011). Focusing on the yellow line, we see that these estimates fluctuate randomly around their mean value, with no apparent trend over time. We take this as an indication that ALG2 and ALG3 are two receivers whose rDCB probably do not show significant variations from epoch to epoch. With this in mind, and considering the two

uppermost lines, we have two key findings. First, the two time series are in good agreement; they both exhibit a variation which is truly apparent on day 17, as an inverted “U-shape” with peak-to-peak range of about 8 nanoseconds. Second, more importantly, most of this variation is in fact a result of temporal variability of rDCB of the ALGO receiver; this has also been confirmed by (Banville and Langley, 2011).

Now let us turn to Figure 2, depicting the rDCB offsets estimated using the MCCL for each of the above three receivers and for day 17 of 2011. These results confirm previous observations that, neither the rDCB of ALG2 nor that of ALG3 is there a significant between-epoch variation; at the same time, ALGO is indeed subject to an apparent intra-day variation in the rDCB, correlated closely with the change in the internal temperature of the receiver (Banville and Langley, 2011).

Figure 3 (Figure 4) shows the results that are analogous to Figure 1 (Figure 2), except using the second set of GPS data. Taken together, we find that, for each receiver considered, the rDCB may not remain stable throughout the course of the three days analyzed. In particular, on day 188, the rDCB of LPGB exhibit a substantial variation, with peak-to-peak range of almost 9 nanoseconds; this fact holds also for the LPGR receiver. Clearly there must be a common cause at work here, which we identify as the temperature perturbations around the antenna shared. At the same time, the LPGS receiver shows a less pronounced intra-day variation in rDCB, reaching a peak-to-peak value of about 4 nanoseconds. These values agree well with what has been found by (Ciraolo et al. 2007).

We carried out four simulation runs, in which we changed the original

values of rDCB of ALG2 receiver on day 17 of 2011. In doing so, we further demonstrate that the MCCL can detect a rDCB variation as small as two nanoseconds (peak-to-peak value), as suggested by Figure 5, showing an excellent agreement between the rDCB offsets estimated (blue line) and the ones simulated (red line) for each simulation run; this agreement, measured in terms of standard deviations from the mean, is at the level approximately 0.5 nanoseconds (or, equivalently, 0.16 meters), and well within the uncertainty of the estimates.

In conclusion, the potential of using the MCCL for detecting the short-term temporal variations of rDCB of a single receiver turns out to be promising.

Analysis of leveling and misspecification errors induced by rDCB variability

We base our analysis of the leveling errors on between-receiver, single-differenced ionospheric observables, associated with two receivers ALGO and ALG2. In the following, for the sake of brevity, we report only the results related to this pair of receivers and to day 17 of 2011, which are representative of all the results that we have obtained.

Figure 6a shows single differences of the CCL-derived ionospheric observables, with each color representing a different arc. Normally, one would expect most arcs will be of at least roughly similar size. However, here we see there is considerable scatter among different arcs, which occurred between 05:00 UTC and 16:00 UTC. In this case, the arc-to-arc scatter reaches a peak-to-peak value of 16 TECu, and taking this value as the estimate of the 95th percentile implies a leveling error of 5.7 TECu. Recall from Figure 2 that,

whereas the rDCB of ALG2 remained relatively stable on day 17, those of ALGO exhibited an apparent variation. Thus, the leveling errors manifesting themselves as arc-to-arc scatter are due to a large extent to intra-day variation in the rDCB of ALGO. This confirms the inability of the CCL to properly handle the short-term temporal variations of rDCB.

Figure 6b is analogous to Figure 6a, except that it shows single differences of the MCCL-derived ionospheric observables. As seen from Figure 6b, the arc-to-arc scatter has been greatly reduced, from nearly 16 TECu (see Figure 6a) to about 4 TECu, resulting in leveling errors that are reasonably small (approximately 1.4 TECu). The reasoning for this is that, with the use of the MCCL, any possible between-epoch variations of rDCB shall fully enter the rDCB offsets that are estimable and thus have no impact on the ionospheric observables retrieved.

In order to assess the misspecification errors, for each receiver we computed two sets of vTEC estimates using, respectively, the CCL- and the MCCL-derived ionospheric observables. Figure 7 shows the ALG2 results. The three panels, from left to right, depict the two sets of vTEC estimates as well as their differences. It follows from this figure that, in this case the first set of vTEC estimates does not deviate, in absolute value, more than 1 TECu from the second set. Hence, as long as the rDCB remain stable, the MCCL performs comparably to the CCL, although it involves more estimable parameters. When it comes to the ALGO results, shown in Figure 8, we extend our findings in two ways. First, as seen from Figure 8a, the CCL results are obviously inaccurate for some time intervals as the vTEC estimates can take negative values, which is rather unrealistic from a practical point of view. The major

reason for this is an apparent intra-day variation in the rDCB of the ALGO receiver, which severely degrades the performance of the CCL and that of the thin-layer ionosphere model, thereby resulting in unreliable vTEC estimates. Second, for the MCCL results shown in Figure 8b, the estimates of the vTEC always take positive values, and in good agreement with those in Figures 7a and 7b (as should be the case), attributable to the ability of the MCCL to deal with rDCB variations. This justifies the use of the MCCL results as ground truth data. On the basis of this, we can conclude that the misspecification errors in the CCL results can range from -5 to 7 TECu, as suggested by Figure 8c.

Conclusions

In this paper, we presented a modified carrier-to-code leveling (MCCL) method, and used S-system theory to construct its full-rank functional model and to analyze the parameter estimability. The contributions of this work cover both the ionospheric observable retrieval, as well as the receiver differential code bias (rDCB) characterization.

In contrast to the original carrier-to-code leveling (CCL) method, the MCCL method proposed can provide ionospheric observables that are less prone to the leveling errors induced by short-term (typically less than one day) temporal variations of rDCB. This holds because the MCCL is different from the CCL in that the former allows the rDCB to be time-varying, while the latter assumes the rDCB to remain invariant over time. This leads to one important practical consequence. With the MCCL one can determine the ionospheric observables interpreted as a combination of the slant total electron content (sTEC), the satellite DCB (considered to be constant over a long period of time, say a day

or a week) and the rDCB at one reference epoch. We investigated the effects that the presence or absence of the intra-day variability of the rDCB have on the quality of the parameters of interest, including not only the ionospheric observables but also the vertical total electron content (vTEC). We showed that the proposed MCCL performs better, or at least comparably, to the customary CCL.

Aside from the ionospheric observables, the estimable parameters that the MCCL can simultaneously provide are rDCB offsets (or better: variations with respect to the reference epoch), thereby enabling us to detect between-epoch fluctuations in the rDCB of a single receiver simply and effectively. The simplicity lies in the fact that, its implementation does not require any special hardware (e.g. simulator) or configuration (e.g. zero or short baseline) support, nor the precise satellite products externally provided. We verified the effectiveness by means of simulation and experimental results, demonstrating its success as a means for characterizing the rDCB variability; therefore, it would be interesting to use the MCCL to disclose information about the short-term temporal variability of rDCB on the International GNSS Service (IGS) permanent stations. This remains to be done as future work. We also plan to strengthen the MCCL model by imposing dynamic constraints on estimable parameters, which is beneficial to (near-) real-time applications, since the rDCB offsets estimated are then expected to have higher precision as well as shorter convergence time.

Acknowledgements

This work was partially funded by the National key Research Program of China

“Collaborative Precision Positioning Project” (No. 2016YFB0501900) and the National Natural Science Foundation of China (Nos. 41604031, 41774042, 41621091). The first author is supported by the CAS Pioneer Hundred Talents Program. The third author acknowledges LU JIAXI International team program supported by the K.C. Wong Education Foundation and CAS.

References

Artru J, Ducic V, Kanamori H, Lognonné P, Murakami M (2005) Ionospheric detection of gravity waves induced by tsunamis. Geophysical Journal International 160(3):840-848

Banville S, Langley RB (2011) Defining the basis of an integer-levelling procedure for estimating slant total electron content. In: Proceedings of the 24th International Technical Meeting of the Satellite Division of The Institute of Navigation (ION GNSS 2011), pp 2542-2551

Banville S, Zhang W, Ghoddousi-Fard R, Langley RB (2012) Ionospheric monitoring using “integer-levelled” observations. In: Proceedings of the 25th International Technical Meeting of the Satellite Division of The Institute of Navigation (ION GNSS 2012), pp 2692-2701

Brunini C, Azpilicueta FJ (2009) Accuracy assessment of the GPS-based slant total electron content .J Geod 83(8):773-785

Brunini C, Azpilicueta F (2010) GPS slant total electron content accuracy using the single layer model under different geomagnetic regions and ionospheric conditions. J Geod 84(5):293-304

Brunini C, Camilion E, Azpilicueta F (2011) Simulation study of the influence of the ionospheric layer height in the thin layer ionospheric model. J Geod 85(9):637

Ciraolo L, Azpilicueta F, Brunini C, Meza A, Radicella S (2007) Calibration errors on experimental slant total electron content (TEC) determined with GPS. J Geod 81(2):111-120

Coster A, Williams J, Weatherwax A, Rideout W, Herne D (2013) Accuracy of GPS total electron content: GPS receiver bias temperature dependence. Radio Sci 48(2):190-196

Dautermann T, Calais E, Haase J, Garrison J (2007) Investigation of ionospheric electron content variations before earthquakes in southern California, 2003–2004. Journal of Geophysical Research: Solid Earth, 2007, 112(B2).

Dettmering D, Limberger M, Schmidt M (2014) Using DORIS measurements for modeling the vertical total electron content of the Earth's ionosphere. J Geod 88(12):1131-1143

Dyrud L, Jovancevic A, Brown A, Wilson D, Ganguly S (2008) Ionospheric measurement with GPS: Receiver techniques and methods. Radio Sci 43(6)

Feltens J (2003) The international GPS service (IGS) ionosphere working group. Adv Space Res 31(3):635-644

Gulyaeva TL, Arikan F, Hernandez‐Pajares M, Veselovsky I (2014) North‐

south components of the annual asymmetry in the ionosphere. Radio Sci 49(7):485-496

Hauschild A, Montenbruck O (2016) A study on the dependency of GNSS pseudorange biases on correlator spacing. GPS Solut 20(2):159-171

Hernández-Pajares M, Juan J, Sanz J (1999) New approaches in global ionospheric determination using ground GPS data. Journal of Atmospheric and Solar-Terrestrial Physics 61(16):1237-1247

Hernández-Pajares M et al. (2009) The IGS VTEC maps: a reliable source of ionospheric information since 1998. J Geod 83(3-4):263-275

Jorgensen P (1978) Ionospheric measurements fromNAVSTAR satellites. Rep. SAMSO-TR-79-29, AD A068809,Def. Tech. Inf. Cent. Cameron Stat., Alexandria, Va

Kao S, Tu Y, Chen W, Weng D, Ji S (2013) Factors affecting the estimation of GPS receiver instrumental biases. Surv Rev 45(328):59–67

Khodabandeh Amir, Teunissen P (2016) Array-aided multifrequency GNSS ionospheric sensing: estimability and precision analysis. IEEE T GEOSCI REMOTE 54(10): 5895-5913

Komjathy A et al. (2012) Detecting ionospheric TEC perturbations caused by natural hazards using a global network of GPS receivers: The Tohoku case study Earth, planets and space 64(12):1287-1294

Komjathy A, Sparks L, Wilson BD, Mannucci AJ (2005) Automated daily processing of more than 1000 ground‐based GPS receivers for

studying intense ionospheric storms. Radio Sci 40(6)

Leick A, Rapoport L, Tatarnikov D (2015) GPS satellite surveying. John Wiley & Sons

Li M, Yuan Y, Zhang B, Wang N, Li Z, Liu X, Zhang X (2017) Determination of the optimized single-layer ionospheric height for electron content measurements over China. J Geod, doi: 10.1007/s00190-017-1054-6

Li Z, Yuan Y, Wang N, Hernandez-Pajares M, Huo X (2015) SHPTS: towards a new method for generating precise global ionospheric TEC map based on spherical harmonic and generalized trigonometric series functions. J Geod 89(4):331-345

Liu Z, Gao Y (2004) Ionospheric TEC predictions over a local area GPS reference network. GPS Solut 8(1):23-29

Mannucci A, Wilson B, Yuan D, Ho C, Lindqwister U, Runge T (1998) A global mapping technique for GPS-derived ionospheric total electron content measurements. Radio Sci 33(3):565-582

Mannucci AJ, Wilson BD, Edwards CD (1993) A new method for monitoring the earth's ionospheric total electron content using the GPS global network. In: Proceedings of ION GPS-93, the 6th international technical meeting of the satellite division of The Institute of Navigation, Salt Lake City, UT, 22–24 September 1993, pp 1323–1332

Park J, von Frese RR, Grejner‐Brzezinska DA, Morton Y, Gaya‐Pique LR (2011) Ionospheric detection of the 25 May 2009 North Korean

underground nuclear test. Geophys Res Lett 38(22)

Sardon E, Rius A, Zarraoa N (1994a) Estimation of the transmitter and receiver differential biases and the ionospheric total electron content from Global Positioning System observations.Radio Sci 29(3):577-586

Sardon E, Rius A, Zarraoa N (1994b) Ionospheric calibration of single frequency VLBI and GPS observations using dual GPS data. J Geod 68(4):230-235

Schaer S (1999) Mapping and Predicting the Earth's Ionosphere Using the Global Positioning System, Ph.D. Dissertation Astronomical Institute, University of Berne, Berne, Switzerland, 25 March

Teunissen P (1985) Zero order design: generalized inverses, adjustment, the datum problem and S-transformations. In: Optimization and design of geodetic networks. Springer, pp 11-55

Wang N, Yuan Y, Li Z, Montenbruck O, Tan B (2016) Determination of differential code biases with multi-GNSS observations. J Geod 90(3):209-228

Wanninger L, Sumaya H, Beer S (2017) Group delay variations of GPS transmitting and receiving antennas. J Geod:1-18

Xue J, Song S, Zhu W (2016) Estimation of differential code biases for Beidou navigation system using multi-GNSS observations: How stable are the differential satellite and receiver code biases? J Geod 90(4):309-321

Zhang B, Ou J, Yuan Y, Li Z (2012) Extraction of line-of-sight ionospheric

observables from GPS data using precise point positioning. Sci China Earth Sci 55(11):1919–1928. doi:10.1007/s11430-012-4454-8

Zhang B, Teunissen PJ (2015) Characterization of multi-GNSS between-receiver differential code biases using zero and short baselines. Sci Bull 60(21):1840–1849

Zhang X, Xie W, Ren X, Li X, Zhang K, Jiang W (2017) Influence of the GLONASS inter-frequency bias on differential code bias estimation and ionospheric modeling. GPS Solut 21(3):1355-1367

Zhong J, Lei J, Dou X, Yue X (2016) Is the long-term variation of the estimated GPS differential code biases associated with ionospheric variability? GPS Solut 20(3):313-319

Zus F, Dick G, Douša J, Heise S, Wickert J (2014) The rapid and precise computation of GPS slant total delays and mapping factors utilizing a numerical weather model. Radio Sci 49(3):207-216

Table 1 An overview of GPS data used in this work

Receiver ID	Receiver type	Antenna type	Longitude, latitude	Observation period
ALGO	(124-U) AOA BENCHMARK ACT 3.3.32.2N	(386) AOAD/M_T NONE	78.07°W, 45.95°N	2011, days 16—18
ALG2	(618-00829) TPS NET-G3A 3.4	(NDE09480005) NOV750.R4 NONE		
ALG3	(401-01989) TPS NETG3 3.4	(383-0414) TPSCR.G3 NONE		
LPGS	(1118) AOA BENCHMARK ACT 3.3.32.2N	(367) AOAD/M_T NONE	57.9°W, 34.9°S	2005, days 188—190
LPGB	NovAtel Millenium	NovAtel 503		
LPGR	NovAtel Millenium			

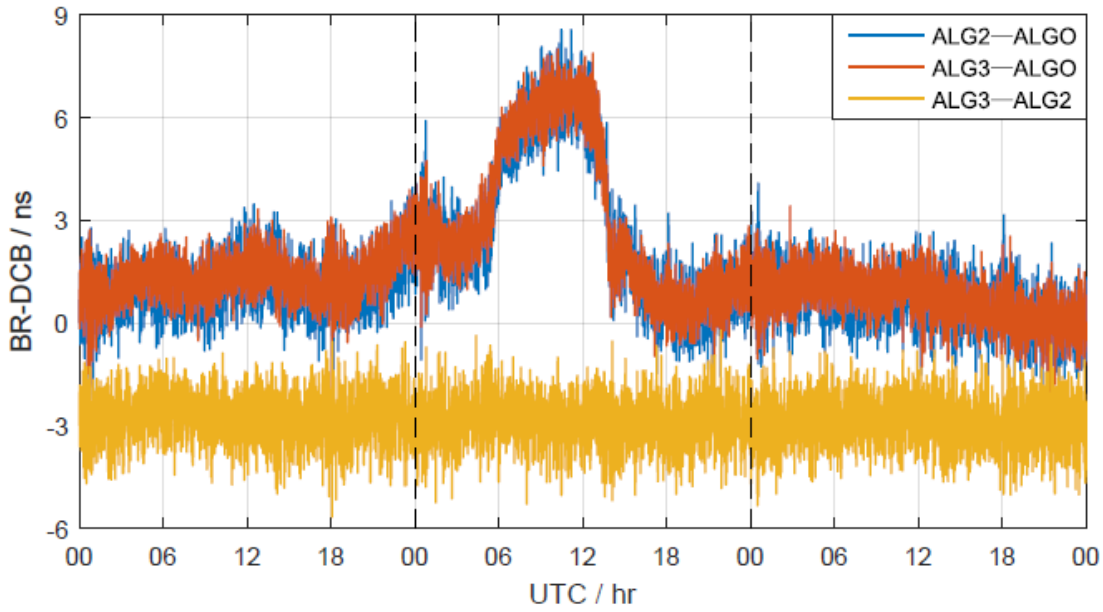

Fig.1 Epoch-by-epoch estimates of BR-DCB for three pairs of receivers (blue line: ALG2—ALGO; red line: ALG3—ALGO; yellow line: ALG3—ALG2. The lines have been arbitrarily shifted vertically for easier interpretation), and for days 16, 17 and 18 of 2011 (Black dash lines show day boundaries).

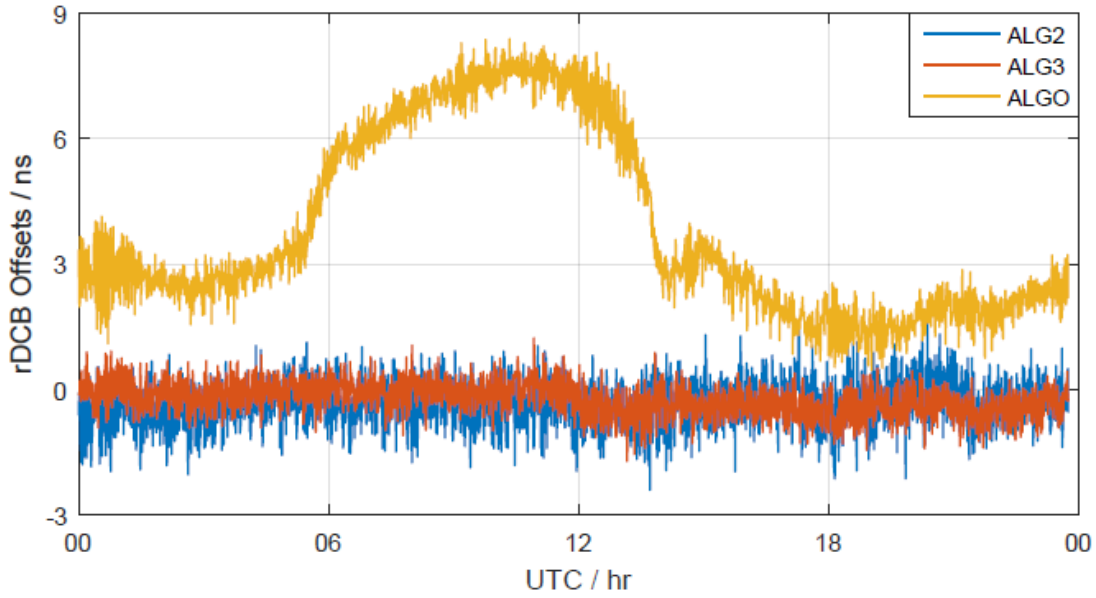

Fig.2 The rDCB offsets estimated using the MCCL for the three receivers ALG2 (blue line), ALG3 (red line) and ALGO (yellow line) on day 17 of 2011. The lines have been arbitrarily shifted vertically for easier interpretation.

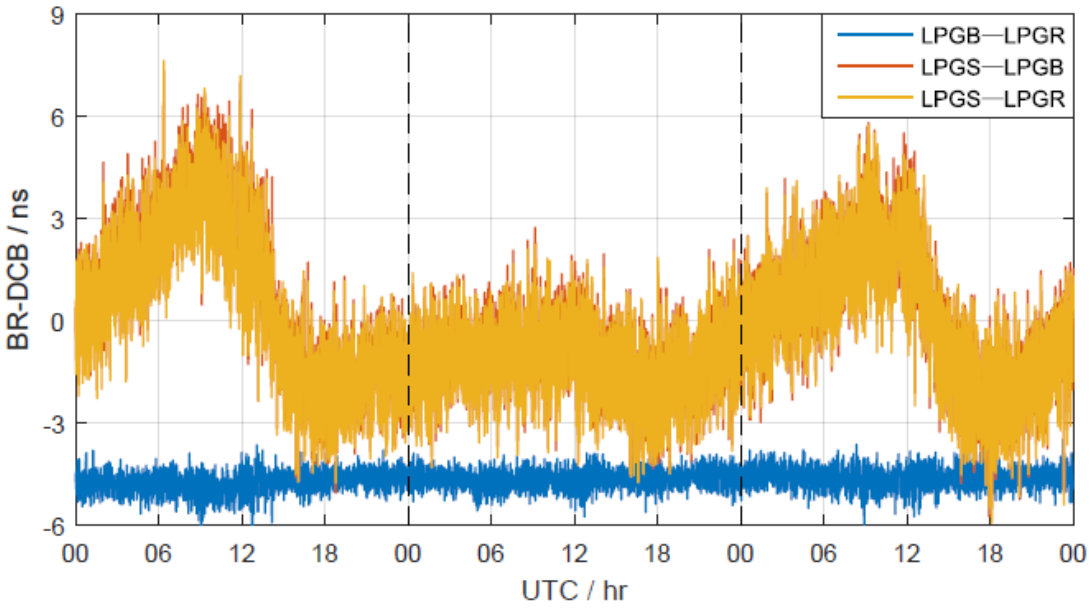

Fig.3 This figure is analogous to Figure 1, except that it shows the results for another three pairs of receivers (blue line: LPGB—LPGR; red line: LPGS—LPGB; yellow line: LPGS—LPGR), and for another three days (188, 189 and 190 of 2005).

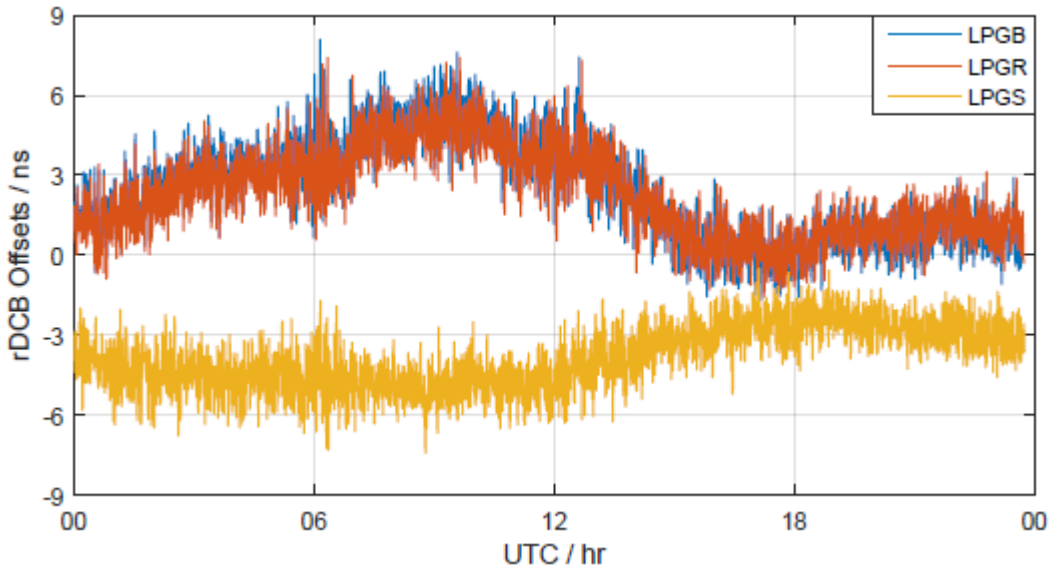

Fig.4 This figure is analogous to Figure 2, except that it shows the results for another three receivers (blue line: LPGB; red line: LPGR; yellow line: LPGS), and for day 188 of 2005.

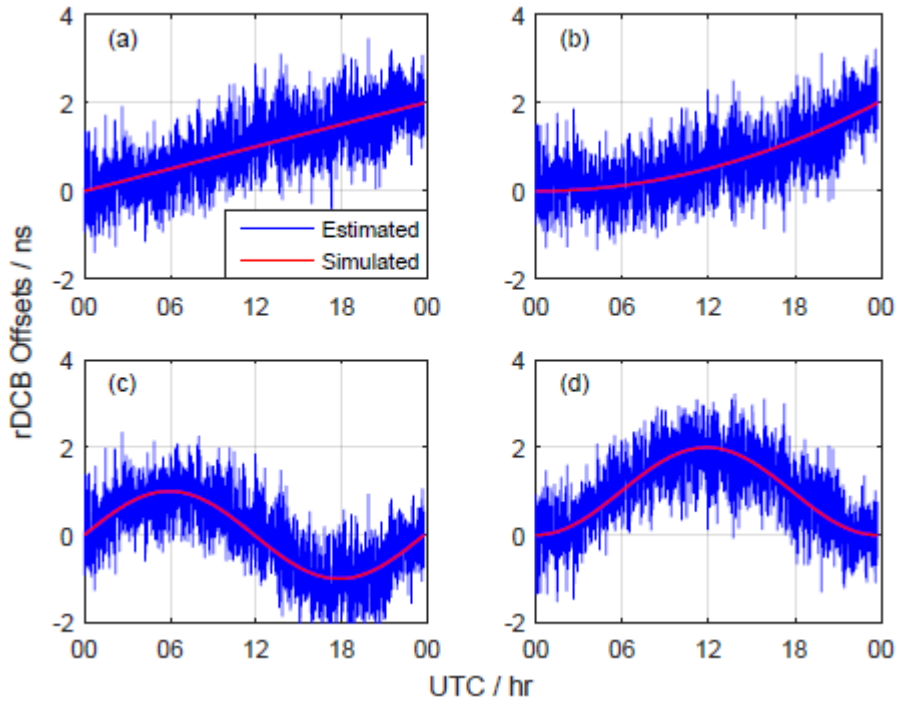

Fig.5 Simulated (red line) versus estimated (blue line) values of rDCB of ALG2 receiver on day 17 of 2011. **a** $y=\frac{2}{T}x$; **b** $y=\frac{2}{T^3}x^3$; **c** $y=\sin\left(\frac{2\pi}{T}x\right)$; **d** $y=1-\cos\left(\frac{2\pi}{T}x\right)$, with $T=2880$ the number of epochs and $x=1\cdots T$ the epoch index.

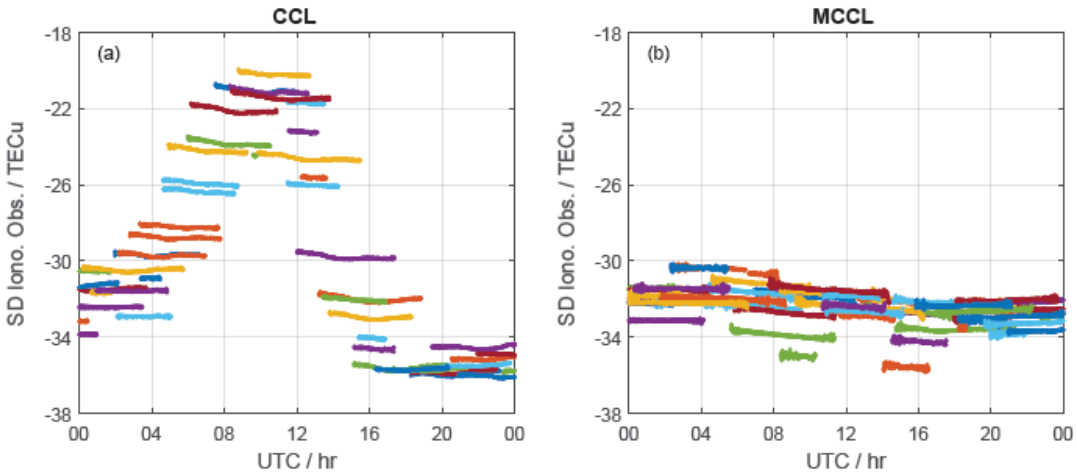

Fig.6 Single differences of ionospheric observables between two receivers ALGO and ALG2 on day 17 of 2011. Each line, colored differently, represents a continuous arc. **a** CCL results; **b** MCCL results

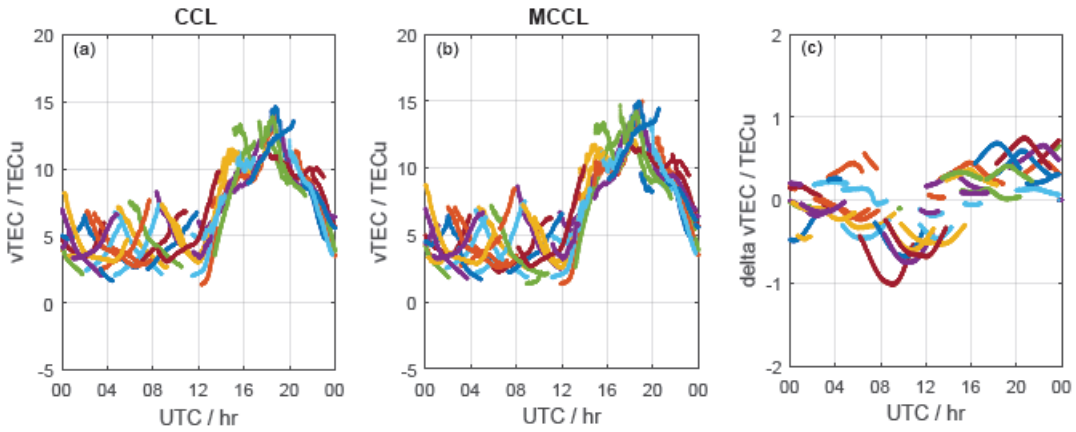

Fig.7 **a** The first set of vTEC, estimated from the CCL-derived ionospheric observables. **b** The second set of vTEC, estimated from the MCCL-derived ionospheric observables. **c** The differences between the first and second sets of vTEC estimates. Different colors correspond to different arcs. These results are associated with the ALG2 receiver and the day 17 of 2011.

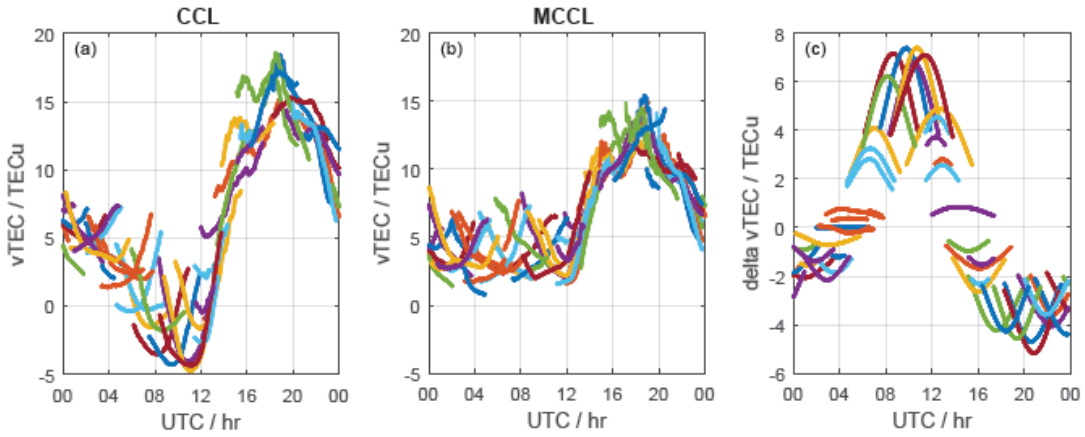

Fig.8 This figure is analogous to Figure 7, except that it shows the results for the ALGO receiver.